How to Understand the Light Curves of Symbiotic Stars

Augustin Skopal
Astronomical Institute, Slovak Academy of Sciences, SK-059 60 Tatranska Lomnica, Slovakia

Received August 13, 2007; revised September 3, 2007; accepted September 4, 2007

Abstract I introduce fundamental types of variations observed in the light curves of symbiotic stars: the orbitally-related wave-like modulation during quiescent phases, eclipses during active phases, and apparent orbital changes indicated during transitions between quiescence and activity. I explain their nature with the aid of the spectral energy distribution of the composite spectrum of symbiotic stars and their simple ionization model.

1. Introduction

The symbiotic stars are understood as interacting binary systems comprising a late-type giant and a hot compact star—most probably a white dwarf. Their orbital periods run usually between one and three years, but can be significantly larger.

Mass loss from the giant represents the primary condition for appearance of the symbiotic phenomenon. A part of the material lost by the giant is transferred to the compact companion via accretion from the stellar wind. This process makes the accretor very hot ($T_h \sim 10^5$ K) and luminous ($L_h \sim 10–10^4$ $L_\odot$), and thus capable of ionizing a fraction of the neutral wind from the giant, giving rise to nebular emission. As a result, the spectrum of symbiotic stars consists of three basic components of radiation—two stellar (from the binary components) and one nebular, emitting by the ionized winds of both the stars.

If the processes of mass-loss, accretion, and ionization are in a mutual equilibrium, then the symbiotic system releases its energy approximately at a constant rate and spectral energy distribution (SED). This stage is known as the *quiescent phase*. Once this equilibrium is disturbed, the symbiotic system changes its radiation significantly, at least in its SED, which leads to a brightening in the optical by a few magnitudes. We call this the *active phase*.

The presence of physically different sources of radiation in the system which differ extremely in temperatures, and also their nature (stellar and nebular component), produce a complex composite spectrum. The resulting spectrum thus depends on the wavelength, the activity of the system, and also the projection of these regions into the line of sight, i.e., on the orbital phase of the binary. In addition, the composite spectrum of individual objects is also a function of their physical and orbital parameters.

Throughout the optical, the light contributions from these sources rival each other, producing a spectrum whose color indices differ significantly from those of standard stars.

Therefore the light curves (LCs) of symbiotic stars have a complex profile, often having an unexpected variation. Generally, the most pronounced changes are observed at the short-wavelength domain of the visual region—namely, within the photometric *U* filter. In this passband the dominant light contribution usually comes from the nebula, which responds most sensitively to the variation of the energy production of the symbiotic system. The large variety of changes recorded in the LCs of symbiotic stars is very broad, and many variations are not quite understood yet. It is, however, clear that they are related to those observed from X-rays to radio wavelengths. From this point of view, photometric monitoring is important to complement other multifrequency observations and thus to help in understanding the responsible physical processes. This aspect was recently highlighted by Sokoloski (2003) and demonstrated for the case of the symbiotic prototype Z And by Sokoloski *et al.* (2006).

In this contribution I discuss just the fundamental types of variations in the LCs of symbiotic stars that reflect most closely their nature—the orbitally-related wave-like variation, eclipses, and apparent changes of the orbital period. To understand these types of variability, I compare the multicolor LCs with the disentangled composite spectrum in the visual domain and consider the basic ionization structure of symbiotic stars. First, I introduce some examples of their LCs.

2. Examples of light curves of well studied symbiotic binaries

2.1. Z Andromedae

Z And is considered a prototype of the class of symbiotic stars. The binary comprises a late-type, M4.5 III giant and a white dwarf accreting from the giant's wind on the 758-day orbit (Nussbaumer and Vogel 1989). More than one hundred years of monitoring Z And has shown the eruptive character of its LC. It displays several active phases, during which fluctuations range in amplitude from a few tenths of a magnitude to about three magnitudes (Formiggini and Leibowitz 1994). Figure 1 (top panel) displays its recent activity from 2000 autumn covering the optical maxima in 2000 December, 2004 September, and 2006 July.

2.2. BF Cygni

BF Cyg is an eclipsing symbiotic binary with an orbital period of 757.2 days (Fekel *et al.* 2001). The system consists of a late-type cool component classified as a normal M5 III giant (Mürset and Schmid 1999) and a hot, luminous compact object (Mikołajewska *et al.* 1989). Its historical LC shows three basic types of active phases—nova-like and Z And type of outburst and short-term flares (Skopal *et al.* 1997). Figure 2 (top panel) shows its LC from 1985 covering the recent 1989 outburst with an eclipse effect and wave-like variation during the following quiescent phase.

2.3 CI Cygni

CI Cyg is also an eclipsing symbiotic binary with an orbital period of 855.25 days

(Belyakina 1979; Belyakina 1984). Its cool component was recently classified as a M5.5 III giant (Mürset and Schmid 1999). A detailed study of this system was made by Kenyon *et al.* (1991). The last major active phase of CI Cyg began in 1975 (Belyakina 1976). During the first four cycles from the maximum, narrow minima indicating eclipses developed in the LC, a typical feature of active phases of symbiotic stars having a high orbital inclination. From 1985 the minima profile became very broad indicating a quiescent phase (Figure 1, mid panel). From 2006 May, CI Cyg entered its new active phase (Skopal *et al.* 2007).

2.4. V1329 Cygni

The symbiotic phenomenon of V1329 Cyg developed during its nova-like eruption in 1964. Prior to this outburst, V1329 Cyg was an inactive star of about 15th magnitude displaying ~2 magnitude-deep eclipses (see Figure 1 in Munari *et al.* (1988)). The post-outburst LC shows large, ~1.5 magnitude deep, periodic, wave-like variations connected with the binary motion. The IUE observations revealed the presence of a strong nebulosity in the near-UV spectrum (Figure 3).

2.5. AG Draconis

This symbiotic system belongs to the group of so-called yellow symbiotics, because it contains a K2 III giant as a cool component (Mürset and Schmid 1999). There are no signs of eclipses either in the optical or the far-UV regions. Schmid and Schild (1997), based on spectropolarimetric observations, derived the orbital inclination i = 60 (± 8.2°). The system undergoes occasional eruptions. The star's brightness abruptly increases by 1–3 magnitudes, often showing multiple maxima separated approximately by one year (Luthardt 1983; Viotti *et al.* 2007). The quiescent phase of AG Dra is characterized by a periodic wave-like variation, which is more pronounced at shorter wavelengths. Figure 2 (mid panel) shows a part of its recent LC covering both the quiescent and the active phases.

2.6. AX Persei

AX Per is known as an eclipsing symbiotic binary with an orbital period of 680 days (Skopal 1991). The cool component of the binary is a normal giant of spectral type M4.5 III (Mürset and Schmid 1999). The historical LC of AX Per is characterized by long-lasting periods of quiescence with the superposition of a few bright stages (see Figure 1 in Skopal *et al.* 2001). Figure 1 (bottom panel) demonstrates evolution in the LC covering a part of its last active phase with eclipses (1990–1994) and the transition to quiescence at 1995.8, followed by typical periodic waves in the star's brightness.

3. Wave-like orbitally-related variation

Wave-like, orbitally related variability represents the most characteristic feature of the LCs of symbiotic stars that develops during their quiescent phases.

Generally, we observe a periodic, wave-like profile of the LC, whose minima and maxima occur at or around conjunctions of the binary components. The inferior conjunction of the giant (the cool component in front of the hot star) corresponds to the light minimum (orbital phase $\varphi = 0$), while at its superior conjunction (the hot star in front) we observe a light maximum ($\varphi = 0.5$). This variation is characterized with a large magnitude difference between the minimum and maximum, $\Delta m \sim 1$–2 magnitudes. This "amplitude" is always larger in the blue part of the spectrum than in the red one, i.e. $\Delta U > \Delta B > \Delta V$. This relationship can be understood with the aid of the SED throughout the *UBV* region.

Figure 2 shows examples of this type of light variation for BF Cyg (it contains a red M5 giant with an effective temperature $T_{eff} \sim 3400$ K) and AG Dra (yellow K2 giant with $T_{eff} \sim 4300$ K) with their SEDs covering the optical domain. This spectral region is dominated by the radiation from the nebula and the giant. The latter does not depend on the orbital phase and strengthens considerably towards the longer wavelengths, while the nebular radiation has the opposite behavior (it dominates the *U* passband and is fainter in *V*) and it is the source of the orbitally-related variation (Section 5.2). Therefore, the Δm amplitudes are declining to longer wavelengths, where the nebular emission is superposed with the increasing light from the giant, which does not vary with the orbital motion.

In other words, the observed amplitude of the wave-like variation is proportional to the ratio of fluxes from the nebula and the giant, which is a function of the wavelength—flux from the giant/nebula increases/decreases with increasing lambda.

In the case of the so-called yellow symbiotic stars (they contain a giant of the spectral type K to G), the giant's contribution into the *V* passband is very strong, which produces very different ΔU and ΔV amplitudes: $\Delta U / \Delta V >> 1$. If the system contains a red giant, its contribution in *V* is relatively lower in the total composite spectrum, which yields the ratio $\Delta U / \Delta V \geq 1$. In our example on Figure 2, $\Delta U / \Delta V$ is ~1.4 for BF Cyg, whereas for the yellow symbiotic star AG Dra, $\Delta U / \Delta V$ is ~10 (see also Figure 25 in Skopal (2005)). On the other hand, a markedly different amplitude in *U* (eventually in *B*) and *V* (eventually in *R*) filters signals the presence of a yellow cool component in the symbiotic system.

4. Eclipses

During the active phases of systems with high orbital inclination, a significant change in the minima profile is observed—the very broad profile becomes narrow. As the minima coincide with the inferior conjunction of the cool component, it is believed that they are caused by eclipses of the hot object by the cool giant. Examples of this effect are shown in Figure 1 and in the top panels of Figure 4 for eclipsing symbiotic binaries BF Cyg, AX Per and CI Cyg.

According to spectroscopic observations, an optically thick shell—a false photosphere—is created around the hot active star, which redistributes a significant fraction of its radiation. As the characteristic temperature of the false photosphere

(~22000 K, Skopal 2005) is considerably lower than that of the hot star during quiescence (~10^5 K), its light contribution will be shifted to longer wavelengths according to Wien's displacement law, and thus make the visual region brighter. The bottom left panel of Figure 4 shows an example of BF Cyg during its 1990 major outburst. The hot star pseudophotosphere radiates at the temperature T_h = 21500 K, and its luminosity contribution is above those from the giant and the nebula through the *UBV* domain. Since the radius of the false photosphere is a few solar radii, the cool giant can eclipse it easily for about one tenth of the orbital period (i.e., 2–3 months) that corresponds to a typical giant's radius of $100R_\odot$ and orbital periods as long as 2–3 years. The depth of eclipses usually obeys the relation: $\Delta U > \Delta B > \Delta V$, because the light from the hot star decreases towards the red part of the spectrum, while that from the giant increases. However, the resulting eclipse depth and color indices are modulated by the presence of a rather strong nebula in the system, which is not subject to eclipses (bottom mid panel of Figure 4). Thus, during totality the nebula partially fills-in the minima and, in combination with the radiation from the giant, produces color indices that differ significantly from those of a normal red giant. For example, we observed $U–V$ ~0, +0.5 and +1.2 for BF Cyg, AX Per, and CI Cyg, respectively, during their total eclipses (compare Figure 4, top). For a comparison, in a theoretical case that the nebula is not present outside the eclipsing giant's stellar disk, we should measure the color indices of a normal red giant, e.g. $U–V$ ~ +3 magnitudes (e.g., Lee 1970).

On the other hand, knowing the spectral type of the giant and having measured magnitudes at totality would allow us to estimate parameters of the contributing nebula—its emission measure and the electron temperature.

During the quiescent phase, radiation from the nebula dominates the optical—its contribution to the *UBV* passbands is well above those from the hot star and the giant (compare Figure 4, bottom right).

The nebula represents a very extended source of radiation in the symbiotic system, which thus cannot be subject to eclipse. As a result, we instead observe a very broad minima; the LC waves as a function of the orbital phase.

5. On the nature of the wave-like variations

5.1. Reflection effect

Originally, Boyarchuk (1966) and Belyakina (1970) suggested a reflection effect as being responsible for the periodic wave-like variation recorded in their LC of AG Peg. In this model, the hot star irradiates and heats up the facing giant's hemisphere that causes variation in the star's brightness when viewing the binary at different orbital phases. The left panel in Figure 5 illustrates the scheme of the reflection effect as suggested by Kenyon (1986). At the inferior conjunction of the giant ($\varphi \sim 0$), we observe a minimum of the light, and conversely, at the giant's superior conjunction ($\varphi \sim 0.5$) we observe its maximum analogous to the Moon's phases.

This natural explanation was adopted by many authors (e.g., Kenyon 1986,

Munari 1989), and it is still considered as a possible cause of the wave variation in LCs as a function of the orbital phase (Munari and Jurdana-Šepić 2002). However, the reflection effect fails to explain quantitatively the observed very large amplitudes of 1–2 magnitudes or more, because a normal red giant does not intercept enough radiation from the hot component to produce the strong emission spectrum and its variation. For symbiotic stars this case was investigated theoretically by Proga *et al.* (1996), who found that the magnitude difference between the illuminated and non-illuminated red giant hemisphere is less than 0.3 magnitude. Also, Skopal (2001) demonstrated that the observational characteristics of the LCs of symbiotic binaries—the large amplitude, the profile of minima, and variation in their positions (see Sect.~5.2)—cannot be reproduced by the reflection effect.

A better agreement between the observed and calculated variation in both the line and the continuum spectrum was achieved by including the neutral wind of the giant into the model, which thus could intercept a much larger amount of the hot star radiation (Proga *et al.* 1998). It became clear that the nature of the orbitally-related changes in the optical/near-UV continuum should be explained within the ionization model of symbiotic binaries, in which the hot star radiation ionizes a portion of the neutral wind from the cool giant.

5.2. Ionization model and the wave-like variability—A simple model

The right panel of Figure 5 shows the ionization structure given by the HII / H I boundaries between the ionized and neutral hydrogen in a symbiotic binary calculated for a gradual acceleration of the giant's wind with the terminal velocity of 20km/s and a steady state case (binary rotation and the gravitational attraction on the wind particles were neglected). The model was originally outlined by Seaquist, Taylor, and Button (1984) (hereafter STB) to explain the radio emission from symbiotic stars and elaborated later by Nussbaumer and Vogel (1987) as a new approach to symbiotic stars to determine their basic physical parameters (Mürset *et al.* 1991; Skopal 2005). The ionization boundary is a curve at which the flux of ionizing photons from the hot star is balanced by the flux of neutral particles (here we consider just hydrogen) from the cool star. In other words, it is defined by the locus of points at which ionizing photons are completely consumed along paths outward from the ionizing star. The shape of the boundary is thus given mainly by the binary properties—separation of the components, number of hydrogen ionizing photons, the mass-loss rate from the giant, and terminal velocity of the wind particles (see in detail Seaquist, Taylor, and Button 1984; Nussbaumer and Vogel 1987).

Figure 5 shows examples of free HII / HI boundaries:

(i) The case when the flux of ionizing photons exceeds significantly that of neutral particles corresponds to a very extended symbiotic nebula—the neutral HI zone has a cone shape with the giant at its top.

(ii) If both the fluxes are approximately equal, dimensions of both the zones are comparable.

(iii) For a very low ionizing capability of the hot star the HII zone can be closed around the hot star.

The SEDs in Figures 2 and 4 demonstrate that the nebula represents a significant source of light in the visual region, mainly during quiescent phases. Figure 5 then suggests that this source of radiation is physically displaced from the giant that excludes directly the reflection effect to be responsible for the orbitally related wave-like variation in LCs. Therefore the principal question is how and why the symbiotic nebula can affect the observed light to explain this type of variability. In the following sections I will try to answer these questions.

5.3. Variation in the nebular emission and LCs

Skopal (2001) found a relationship between the wave-like variation in LCs and the radiation from the symbiotic nebula. Both dependencies are of the same type. We observe a maximum/minimum of the nebular emission around the conjunctions of the binary components, similar to the periodic, wave-like variation of the photometric magnitudes. Figure 3 demonstrates this case for V1329 Cyg (Section 2.4). Maximum/minimum of the nebular emission at $\varphi = 0.57 / 0.95$ (bottom panels) corresponds to the maximum/minimum in the LC (top).

Thus, the orbitally-related variation in the nebular component of radiation causes that which is observed in the LCs. This relationship can be verified by converting the observed amount of the nebular radiation, usually characterized by the emission measure, EM, to the scale of magnitudes. (Note: The flux produced by the nebula of a volume *V* with concentrations of ions (protons), n_+, and electrons, n_e, largely depends on the number of hydrogen recombinations, and is proportional to $\int n_+ n_e \, dV$—the so-called emission measure.) Under the assumption that the light from the nebula dominates the considered passband, which is usually satisfied for *U*, the stellar magnitude, for example, m_U, can be expressed as

$$m_U = -2.5 \log (EM) + C_U, \qquad (1)$$

where the constant C_U depends on the volume emission coefficient and the contribution of the zero magnitude star in *U* (see in detail Skopal 2001). Figure 3 shows a very good agreement between the *B*-magnitudes determined according to Equation (1) and those obtained by standard photometric measurements.

This result thus confirms the unambiguous connection between variations in the nebular emission and photometric measurements.

5.4. Why does the emission measure vary?

It is simple to imagine that the orbitally-related variations in the nebular emission are only apparent. This implies that a fraction of the nebular medium has to be partially optically thick to produce different contributions of its total emission into the line of sight at different orbital phases.

Within the STB model the opacity, κ, of the ionized emission medium decreases with the distance *r* from the giant, since $\kappa \propto \text{density}(r) \propto r^{-2}$. This implies that the parts

of the nebula closest to the boundary between the stars will be the most opaque.

In the case of the extensive emission zone, the optically thick portion of the HII region has the geometry of a canopy located on the boundary around the binary axis (Figure 5, right). Such a shape will attenuate most of the radiation at orbital phase 0 (i.e., the relatively largest part of the optically thin nebula will be obscured by it), while at phase 0.5, we will observe a maximum light from the nebula in agreement with the variation in EM and the LCs. In this case the LC profile will be a simple sinusoid.

In the case of an oval shape of the HII zone (Figure 5, the dotted curve) its total emission will be attenuated more at positions of the binary component's conjunctions (the orbital phases $\varphi = 0$ and 0.5) than at positions of $\varphi = 0.25$ and 0.75, when viewing the binary from its sides. Such apparent variation in the EM can produce the primary, but also a secondary minimum in the LC. The secondary minima of this nature are well demonstrated by the *U*–LC of EG And (see Figure 2 in Skopal 2005).

The above described approximation of the nebula shaping in a symbiotic system allow us to explain qualitatively just the most pronounced features of the LCs. A more accurate ionization structure, including the effect of the binary rotation and the gravitational attraction on the wind particles, has not been investigated yet. Nevertheless, an asymmetry of the nebula with respect to the binary axis (i.e., the line connecting the stars) can be indicated observationally. The recently discovered effect of apparent changes in the orbital period gives evidence of this possibility.

6. Apparent changes in the orbital period

This effect is connected with transitions between the active and quiescent phases of a symbiotic system. Aside from the significant change of the minima profile during these periods (Section 4, Figure 4), a systematic variation in the minima position, i.e., the effect of apparent orbital changes, was revealed (Skopal 1998).

6.1. Systematic variation in the O–C residuals

Here I will demonstrate this effect on the historical LC of the eclipsing symbiotic system BF Cyg (Figure 6). First, we determine positions of the observed ("O") minima in its LC and calculate those ("C") using a reference ephemeris. Then we construct the so-called O–C diagram (i.e., the residuals between the observed and calculated timing of the minima). In our example of BF Cyg the O–C diagram was constructed using the reference ephemeris given by all the primary minima measured by Skopal (1998):

$$JD_{Min} = 2411268.6 + 757.3(\pm 0.6) \times E, \qquad (2)$$

which is identical (within uncertainties) with the spectroscopic ephemeris of Fekel *et al.* (2001).

A systematic variation in the O–C residuals is clearly seen. This behavior was already noted by Jacchia (1941). The gradual increase of the O–C values before the 1920 bright stage (E = 1 to 11) corresponds to an apparent period of 770 days, larger

than the orbital one, while their subsequent decrease (E = 12 to 24) indicates a shorter period of 747 days.

The same type of variability appeared again during the recent, 1989 active phase. Observed changes in both the position and the shape of the minima are illustrated in the top left panel of Figure 4, and in Figure 6. During the transition *from the active phase to quiescence* (A → Q transitions), a systematic change in the minima positions at E = 49 to 51 corresponded to the apparent period of only 730 days.

During the transition *from the quiescent to the active phase* (Q → A transitions), a significant change in the O–C values by a jump of +130 days was observed. The minima positions at E = 47 and E = 49 indicate an apparent period of 822 days.

6.2. Asymmetric shape of the HII zone

To explain the observed apparent changes in the orbital period, the HII zone has to be extended asymmetrically with respect to the binary axis. Asymmetrical shape of the ionized region in symbiotic stars was also suggested, for example, by:

(i) spectropolarimetric studies of Schmid (1998) and

(ii) hydrodynamical calculations of the structure of stellar winds in symbiotic stars that include effects of the orbital motion (e.g., Folini and Walder 2000).

In both models the ionization front in the orbital plane is twisted, going from the side of the hot star that precedes its orbital motion, through the line joining the components, to the front of the cool star against its motion. Therefore, it is possible to assume that the main nebular region follows the S-shaped track from the front of the hot star orbital motion to the binary axis. Thus, the optically thick fraction of the HII region is prolonged so that its major axis at the orbital plane points the observer around the orbital phase 0.9.

6.3. Principle of apparent orbital changes

During the A → Q transitions, the optically thick shell is gradually diluting, which leads to the increase of the hot star temperature and thus production of the ionizing photons. As a result, the nature of the optical continuum declines and changes significantly—from blackbody to nebular radiation (Figure 4, bottom left and right panel). This process causes an *expansion* of the HII zone and thus the change of the minimum profile from narrow to broad wave throughout the orbital cycle. According to the asymmetry of the nebula (Section 6.2) the light minima occur prior to the time of spectroscopic conjunction. This behavior is also illustrated by the top panels of Figure 4. Thus, during the A → Q transitions we indicate an apparent period, which is *shorter* than the orbital one.

During Q → A transitions a sudden decrease in the luminosity of the ionizing photons results from rather rapid creation of the false relatively cool photosphere. This implies a disruption of the HII zone. The optical region is then (usually) dominated by the stellar radiation from the pseudophotosphere and a narrow minimum (eclipse) is observed at the inferior conjunction of the giant. In such a case

the time difference between the preceding broad minimum ($\varphi \approx 0.9$) and the eclipse ($\varphi \approx 0$) is $P_{app} \approx P_{orb} + 0.1 \times P_{orb}$. This apparent change in the period happens suddenly, and in the O–C diagram is indicated by a jump in the residuals. In our illustration of BF Cyg (Figure 6, minima just prior to the 1989 outburst), the timing of the broad minimum at the epoch E = 47 and the following eclipse at E = 49 corresponds to the apparent period $P_{app} \approx 822$ days.

7. Concluding remarks

7.1. A complexity of LC profiles

We have discussed only the fundamental variations in the LCs of symbiotic stars, i.e., those that can be explained with the aid of a basic model. However, LCs of symbiotic stars record a much larger variety of light changes that are unexpected and never repeat again. For example, during quiescence the wave-like variation is not a simple sinusoid, but alters its profile from cycle to cycle in both scales—time and brightness (e.g., EG And, AG Peg, AX Per, see Skopal *et al.* 2007). During active phases the LC profiles are very heterogeneous. Eruptions arise unexpectedly with a rapid increase (e.g., RS Oph and most of AG Dra events), or more frequently with a gradual increase to the maximum within a few months (e.g., recent outbursts of Z And and AG Dra (Skopal *et al.* 2006; Skopal *et al.* 2007)). Also the recurrence time is an unpredictable phenomenon. For some objects no active phase has yet been recorded (e.g., SY Mus, RW Hya, EG And). For others, eruptions are scattered in historical LCs irregularly. For example, during the 1994–1998 period the AG Dra LC (Figure 2) showed eruptions with a strict recurrence of ~1 year (Viotti *et al.* 2007).

Previously, Iijima *et al.* (1987) suggested that since 1930 AG Dra periodically entered active stages with an interval of about 15 years. However, from the beginning of its historical records of the brightness from 1890 to about 1927, it was quiet with a first strong outburst indicated around 1932 (Robinson 1969). Another illustrative example in this respect is YY Her (Munari *et al.* 1997). In addition, an even more complex profile of the LC is observed when different types of eruptions (nova-like, Z And-type, flares) are superposed. An example here is the historical LC of BF Cyg (Figure 6; see Skopal *et al.* 1997).

7.2. The problem of eclipses

Eclipses can suddenly arise in the LC during active phases of symbiotics with a high orbital inclination (Section 4). However, their presence is not stable during each outburst of some symbiotic objects. For example, evidence for eclipses in the symbiotic triple system CH Cyg were reported by Skopal *et al.* (1996). However, those produced by the inner symbiotic binary were observed only during the lower level of the activity (1967–1971 and 1992–1995).

Generally, the depth of eclipses is very sensitive to the location of the main sources of radiation in the system and their relative contributions at the considered passband, which both can be subject to variation during different active phases.

Therefore the eclipse effect can be observed only at specific brightness phases, at which the radiative contribution from a pseudophotosphere in the optical rivals that of the nebula. In addition, in the the case of CH Cyg, the effect of the precession of the inner orbit (i.e., that with the symbiotic pair) with a period of 6,520 days and the precession cone opening angle of 35° (Crocker *et al.* 2002) is probably the main cause of the intriguing behavior of eclipses in this system.

An additional problem connected with eclipses in symbiotic binaries is their width. In some cases it is too large to be explained by a simple eclipse of the hot object by the stellar disk of the giant. Examples here are BF Cyg (Skopal *et al.* 1997) and TX CVn (Skopal *et al.* 2007). In the case of Z And the broad eclipse profile suggested a disk-like structure for the hot object during active phases (Skopal 2003).

7.3. Importance of the photometric monitoring

The diversity of variations recorded in the LCs of symbiotic stars is thus far beyond our full understanding. The investigation of interactions between the cool giant and its hot luminous compact companion in a symbiotic binary requires simultaneous, multi-frequency observations from X-rays to radio wavelengths. This is an extremely challenging task, addressed mainly to large ground-based telescopes and those on satellites.

In spite of this, the photometric monitoring of symbiotic stars, usually carried out with small telescopes, plays an important role in such research. I summarize some reasons as follows:

(i) Monitoring usually first discovers an unpredictable sudden change in the brightness and thus can provide an alert for observation with other facilities.

(ii) Color indices can provide information about the nature of the composite continuum and thus to help to identify the responsible process.

For example, the very negative intrinsic (i.e., dereddened and corrected for lines) *U–B* index is usually connected with optical brightening that signals the energy conversion from the hot star to the nebular emission. Some examples were discussed by Skopal *et al.* (2006) and Tomov *et al.* (2004).

(iii) The eclipse profiles can help to recognize the structure of the hot active object—a spherical or a disk-like structure. Disentangling the color indices during the totality allows us to quantify the contribution from the non-eclipsed fraction of the nebula (Section 4).

(iv) The minima during quiescence, whose profiles reflect the geometry of the nebula, can determine the difference between the simplified ionization structure (compare Figure 4) and the real situation including effects of the binary motion and accretion.

(v) Variation in the LC profile in the *UB*[*V*] bands around the orbital phase $\varphi \sim 0.5$ (e.g., presence/absence of a secondary minimum) can probe the extension of the nebula—if it is closed or open in the sense of the STB model (Figure 5, Section 5.2).

(vi) A double-wave profile in the [*V*]*RI* passbands implies the possibility of the ellipsoidal shape of the red giant due to tidal distortion and thus can discriminate the type of mass transfer process (via the wind or the Roche lobe overflow?).

(vii) An intrinsic variability of the giant component in symbiotic binaries monitored in the *VRI* passbands can provide physical parameters for such "pulsation-type" of variability. Objects as CH Cyg, CI Cyg, AG Peg, and AR Pav are promising candidates here (Mikołajewski *et al.* 1992; Belyakina and Prokofieva 1991; Skopal *et al.* 2007; Skopal *et al.* 2000).

(viii) Multicolor LCs, if properly corrected for influence of emission lines (Skopal 2007), can provide a satisfactory tool to calibrate spectroscopic observations and thus be useful in determining other physical parameters.

(ix) Evolution in the LC profile at the very beginning stage of outbursts is of particular importance to mapping the process igniting the eruption (e.g., Sokoloski *et al.* 2006).

8. Acknowledgements

This work was supported by the Slovak Academy of Sciences grant No. 2/7010/7.

References

Belyakina, T. S. 1970, *Astrofizika*, **6**, 49.
Belyakina, T. S. 1976, *Inf. Bull. Var. Stars*, No. 1169.
Belyakina, T. S. 1979, *Izv. Krymskoj Astrofiz. Obs.*, **59**, 133.
Belyakina, T. S. 1984, *Izv. Krymskoj Astrofiz. Obs.*, **68**, 108.
Belyakina, T. S. 1992, *Izv. Krymskoj Astrofiz. Obs.*, **84**, 49.
Belyakina, T. S., and Prokofeva, V. V. 1991, *Astron. Zh.*, **68**, 314.
Boyarchuk, A. A. 1966, *Astron. Zh.*, **43**, 976.
Crocker, M. M., Davis, R. J., Spencer, R. E., Eyres, S. P. S., Bode, M. F., and Skopal, A. 2002, *Mon. Not. Roy. Astron. Soc.*, **335**, 1100.
Fekel, F. C., Hinkle, K. H., Joyce, R. R., and Skrutskie, M. F. 2001, *Astron. J.*, **121**, 2219.
Folini, D., and Walder, R. 2000, *Astrophys. Space Sci.*, **274**, 189.
Formiggini, L., and Leibowitz, E. M. 1994, *Astron. Astrophys.*, **292**, 534.
Iijima, T., Vittone, A., and Chochol, D. 1987, *Astron. Astrophys.*, **178**, 203.
Jacchia, L. 1941, *Bull. Harvard Coll. Obs.*, No. 915.
Kenyon, S. J. 1986, *The Symbiotic Stars*, Cambridge Univ. Press, Cambridge, p. 27.
Kenyon, S. J., Oliversen, N. A., Mikołajewska, J., Mikołajewski, M., Stencel, R. E., Garcia, M. R., and Anderson, C. M. 1991, *Astron. J.*, **101**, 637.
Lee, T. A. 1970, *Astrophys. J.*, **162**, 217.
Luthardt, R. 1983, *Mitt. Veränderliche Sterne*, **9**, 129.
Mikołajewska, J., Mikołajewski, M., and Kenyon, S. J. 1989, *Astron. J.*, **98**, 1427.

Mikołajewski, M., Mikołajewska, J., and Khudyakova, T. N. 1992, *Astron. Astrophys.*, **254**, 127.
Munari, U. 1989, *Astron. Astrophys.*, **208**, 63.
Munari, U., and Jurdana-Šepić, R. 2002 *Astron. Astrophys.*, **386**, 237.
Munari, U., Margoni, R., and Mammano, A. 1988, *Astron. Astrophys.*, **202**, 83.
Munari, U., *et al.* 1997, *Astron. Astrophys.*, **323**, 113.
Mürset, U., Nussbaumer, H., Schmid, H. M., and Vogel, M. 1991, *Astron. Astrophys.*, **248**, 458.
Mürset, U., and Schmid, H. M. 1999, *Astron. Astrophys., Suppl. Ser.*, **137**, 473.
Nussbaumer, H., and Vogel, M. 1987, *Astron. Astrophys.*, **182**, 51.
Nussbaumer, H., and Vogel, M. 1989, *Astron. Astrophys.*, **213**, 137.
Proga, D., Kenyon, S. J., and Raymond, J. C. 1998, *Astrophys. J.*, **501**, 339.
Proga, D., Kenyon, S. J., Raymond, J. C., and Mikołajewska, J. 1996, *Astrophys. J.*, **471**, 930.
Robinson, L. 1969, *Perem. Zvezdy*, **16**, 507.
Schmid, H. M. 1998, *Rev. Mod. Astron.*, **11**, 297.
Schmid, H. M., and Schild, H. 1997, *Astron. Astrophys.*, **321**, 791.
Seaquist, E. R., Taylor, A. R., and Button, S. 1984, *Astrophys. J.*, **284**, 202.
Skopal, A. 1991, *Inf. Bull. Var. Stars*, No. 3603.
Skopal, A. 1998, *Astron. Astrophys.*, **338**, 599.
Skopal, A. 2001, *Astron. Astrophys.*, **366**, 157.
Skopal, A. 2003, *Astron. Astrophys.*, **401**, L17.
Skopal, A. 2005, *Astron. Astrophys.*, **440**, 995.
Skopal, A. 2007, *New Astron.*, **12**, 597.
Skopal, A., Bode, M. F., Lloyd, H., and Tamura, S. 1996, *Astron. Astrophys.*, **308**, L9.
Skopal, A., Djuraševič, G., Jones, A., Drechsel, H., Rovithis-Livaniou, H., and Rovithis, P. 2000, *Mon. Not. Roy. Astron. Soc.*, **311**, 225.
Skopal, A., Teodorani, M., Errico, L., Vittone, A. A., Ikeda, Y., and Tamura, S. 2001, *Astron. Astrophys.*, **367**, 199.
Skopal, A., Vaňko, M., Pribulla, T. *et al.* 2007, *Astron. Nachr.*, **328**, 909.
Skopal, A., Vittone, A., Errico, L., Bode, M. F., Lloyd, H. M., and Tamura, S. 1997, *Mon. Not. Roy. Astron. Soc.*, **292**, 703.
Skopal, A., Vittone, A. A., Errico, L., Otsuka, M., Tamura, S., Wolf, M., and Elkin, V. G. 2006, *Astron. Astrophys.*, **453**, 279.
Sokoloski, J. L. 2003, *J. Amer. Assoc. Var. Star Obs.*, **31**, 89.
Sokoloski, J. L., *et al.* 2006, *Astrophys. J.*, **636**, 1002.
Tomov, N. A., Tomova, M. T., and Taranova, O. G. 2004, *Astron. Astrophys.*, **428**, 985.
Viotti, R. F., Friedjung, M., González-Riestra, R., Iijima, T., Montagni, F., and Rossi, C. 2007, *Baltic Astron.*, **16**, 20.

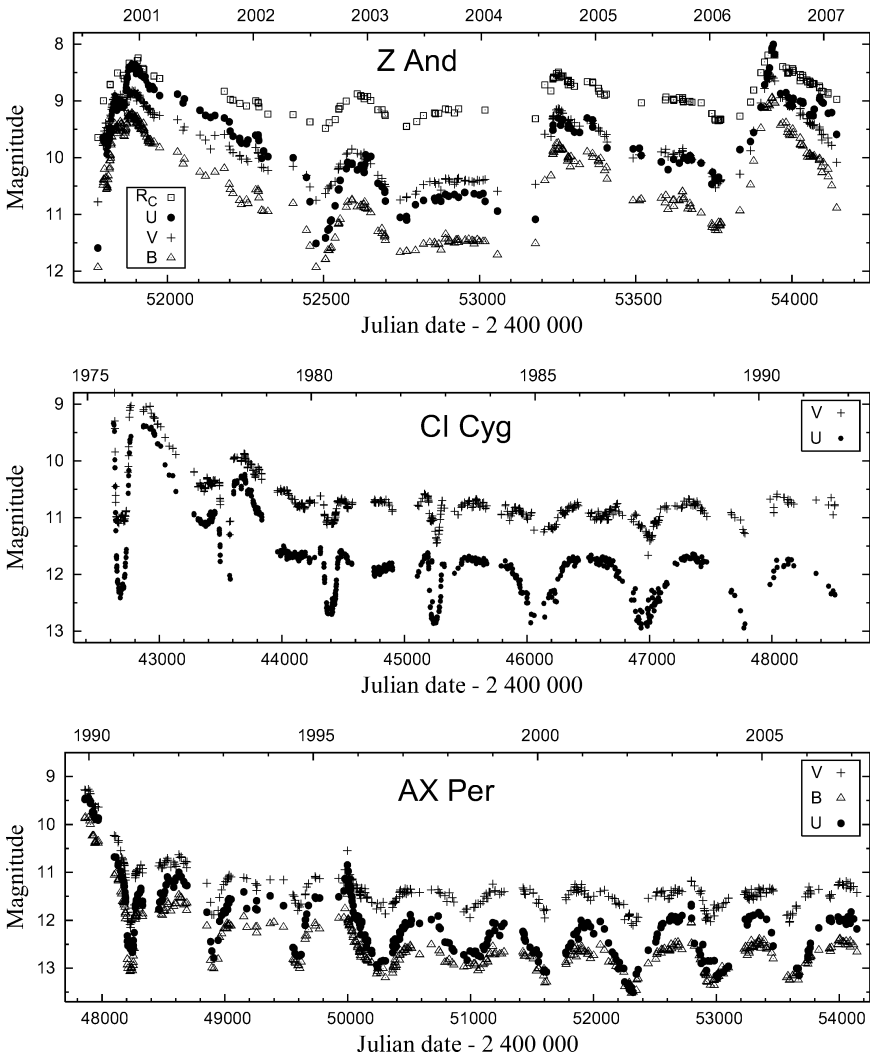

Figure 1. Top: The $UBVR_C$ LCs of Z And covering two major eruptions that peaked in 2000 December and 2006 July (from Skopal *et al.* 2007). Middle: Example of *U* and *V* LCs of CI Cyg from its 1975 outburst with narrow minima—eclipses. From about 1984 eclipses transferred into wave-like variation signaling thus quiescent phase. The data are from Belyakina (1992). Bottom: The *UBV* LCs of AX Per covering a part of its 1989–1994 active phase and the following quiescence from 1995 (see Skopal *et al.* 2001).

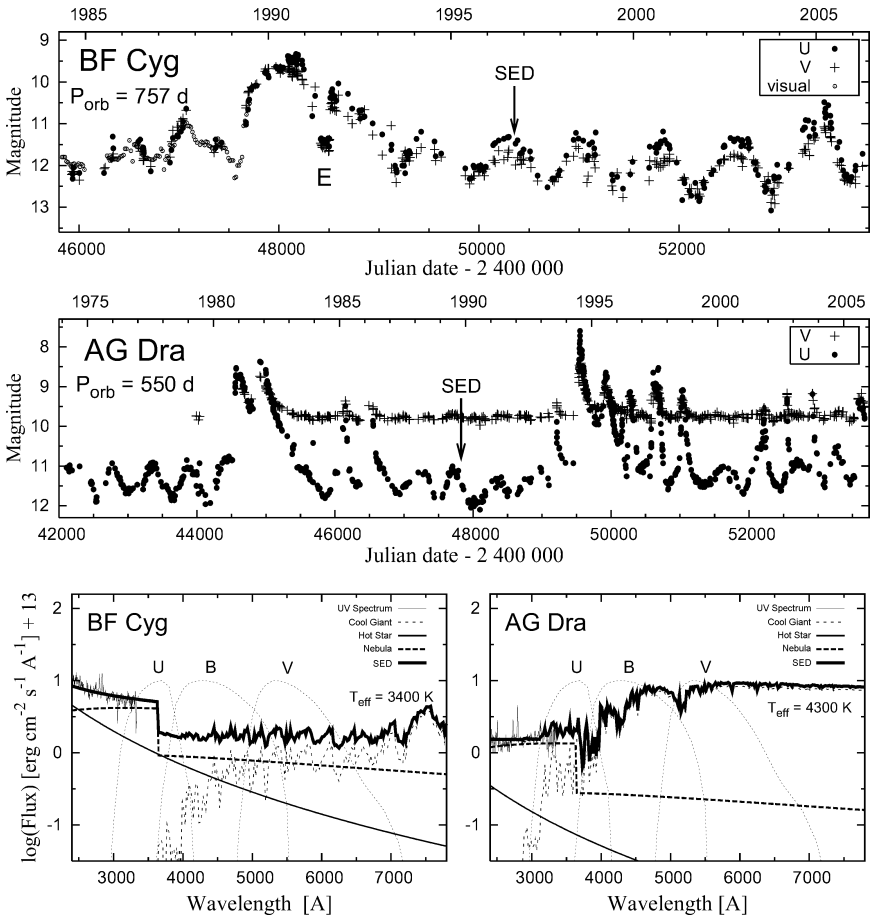

Figure 2. Top panels show the LCs of BF Cyg and AG Dra in *U* and *V* filters. During active phase the eclipsing system BF Cyg displays a relatively narrow minimum at the inferior conjunction of the giant (denoted by "E"), while during quiescent phase its LC shows pronounced wave-like variation, characterized with amplitudes $\Delta U \approx \Delta V \sim 1.5$ mag. The yellow symbiotic star AG Dra is not eclipsing. Amplitudes of its wave-like variations are smaller and depend considerably on the color: $\Delta U \sim 1$ mag, $\Delta V \sim 0.1$ mag. The bottom panels show the SEDs of these objects throughout the *UBV* passbands, which explains the observed differences in the wave-like variation (Section 3).

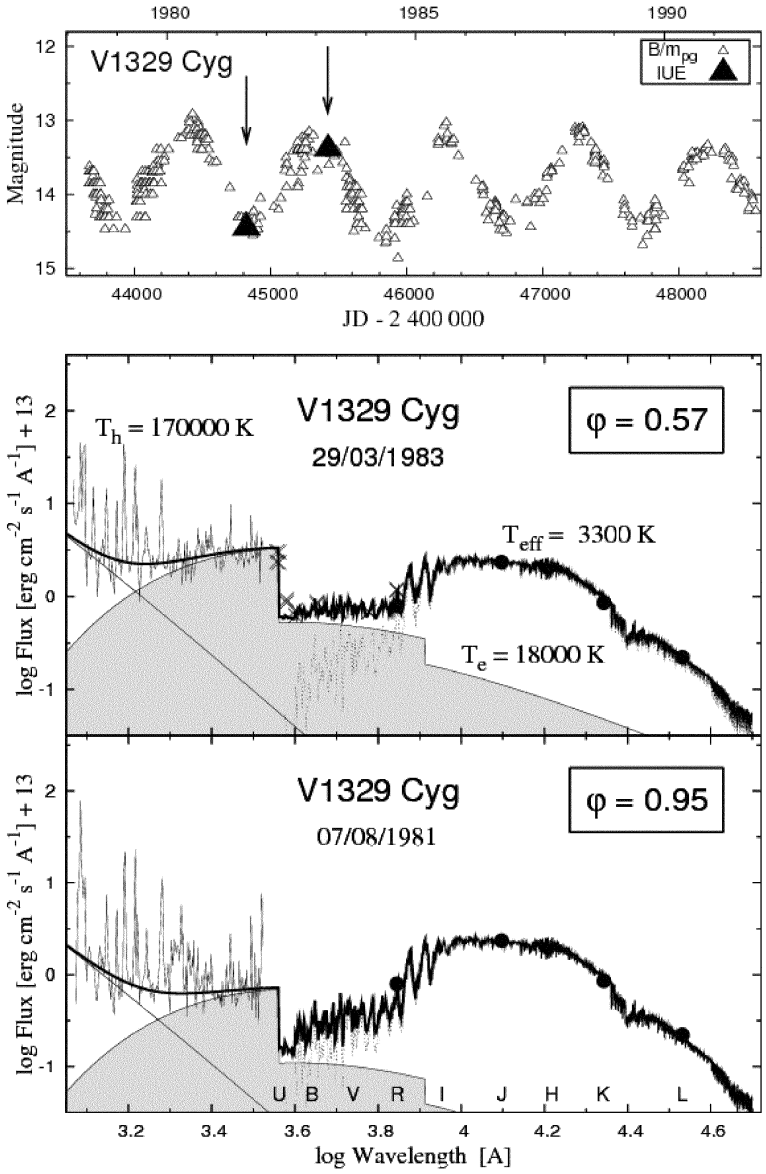

Figure 3. Example of the wave-like, orbitally-related variation in the LC of V1329 Cyg during quiescent phase (top). It is caused by variation in the quantity of the nebular radiation observed at different orbital phases (bottom panels). Magnitudes derived from the IUE spectra agree perfectly with those obtained photometrically (filled triangles in the top panel). This result thus demonstrates that the periodic variation in the nebular radiation is responsible for that observed in the LCs.

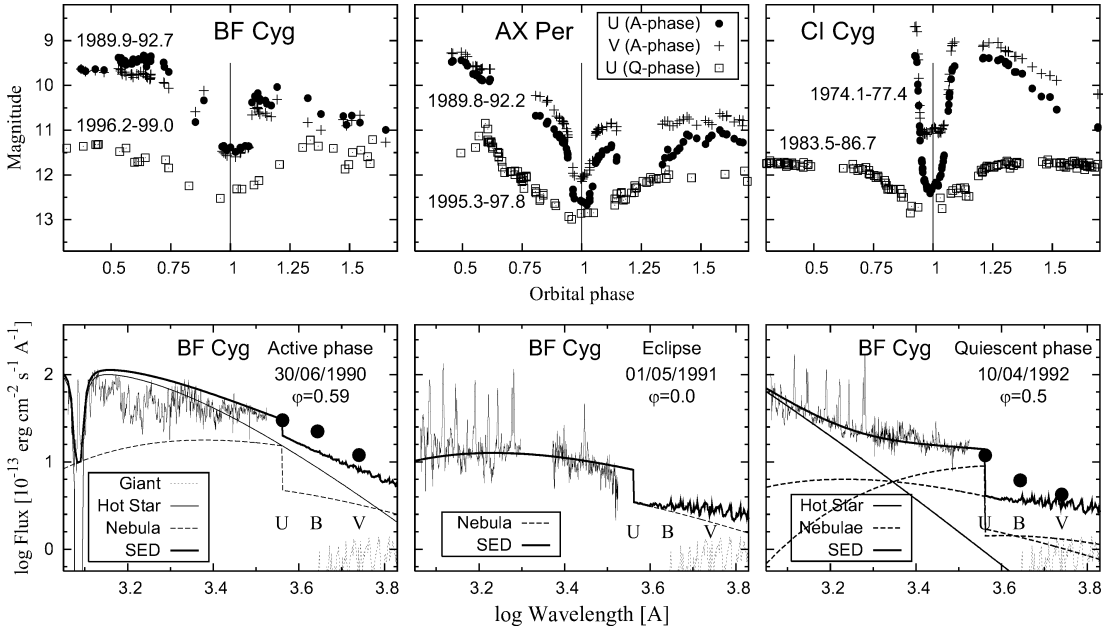

Figure 4. Eclipses + wave variation and SEDs. Bottom: Examples of the SED during the active phase (left panel), eclipse (middle) and quiescent phase (right) of BF Cyg. During activity contribution from a warm false photosphere around the hot star is larger than that from the nebula in the *UBV* region. As a result we observe narrow minima—eclipses—in the LC at the inferior conjunction of the giant. The minima are in part filled in with rather strong residual light from the nebula, which is not subject to eclipse (mid panel). During quiescence the radiation from extended nebula(e) dominates the UBV region (right panel), which causes the minima to be very broad. Top panels demonstrate how these SED variations are reflected by the LCs of eclipsing systems BF Cyg, AX Per, and CI Cyg.

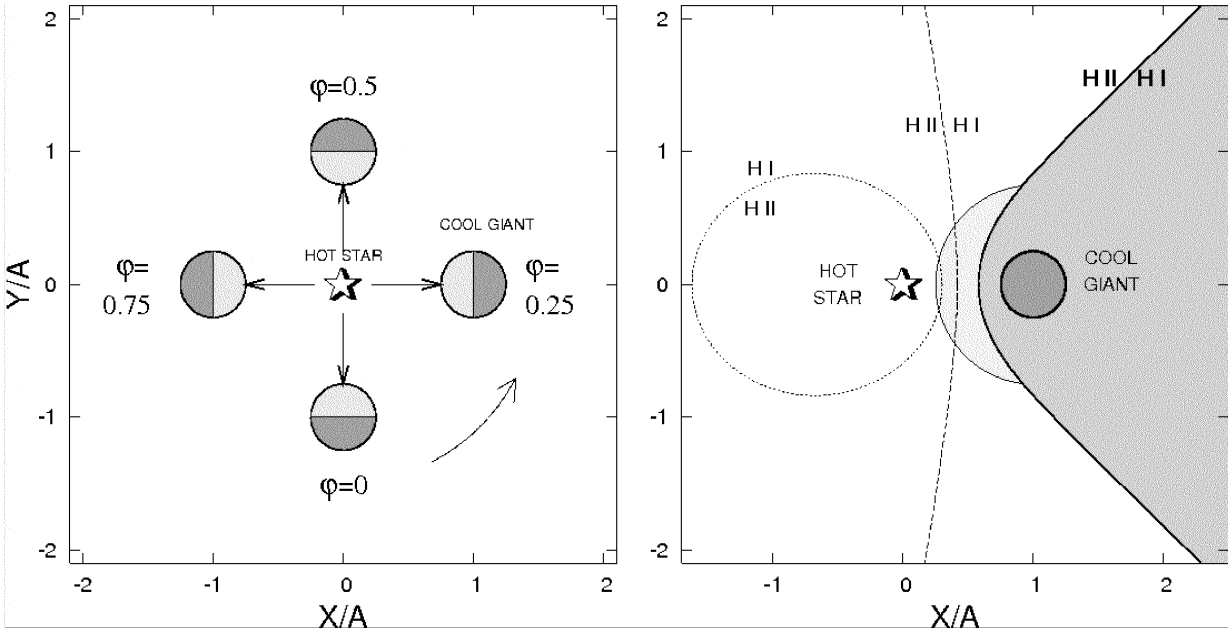

Figure 5. Left: Schematic representation of the reflection effect. Within this model the wave-like, orbitally-related variation in LCs of symbiotic stars results from different visibility of the illuminated giant's hemisphere (the lighter one facing the hot star) at different phases. This model, however, neglects the effect of ionization of the neutral wind from the giant. Right: The STB (1984) ionization structure of the hydrogen in symbiotic binary. The boundary between the ionized and neutral hydrogen (HII / HI) for a strong (heavy solid line), moderate (dashed line), and faint (dotted line) source of the ionizing photons (i.e., the hot star). Within this model the wave-like variability results from a different projection of the optically thick portion of the ionized zone (the light gray part of the HII zone) into the line of sight (see Section 5.2).

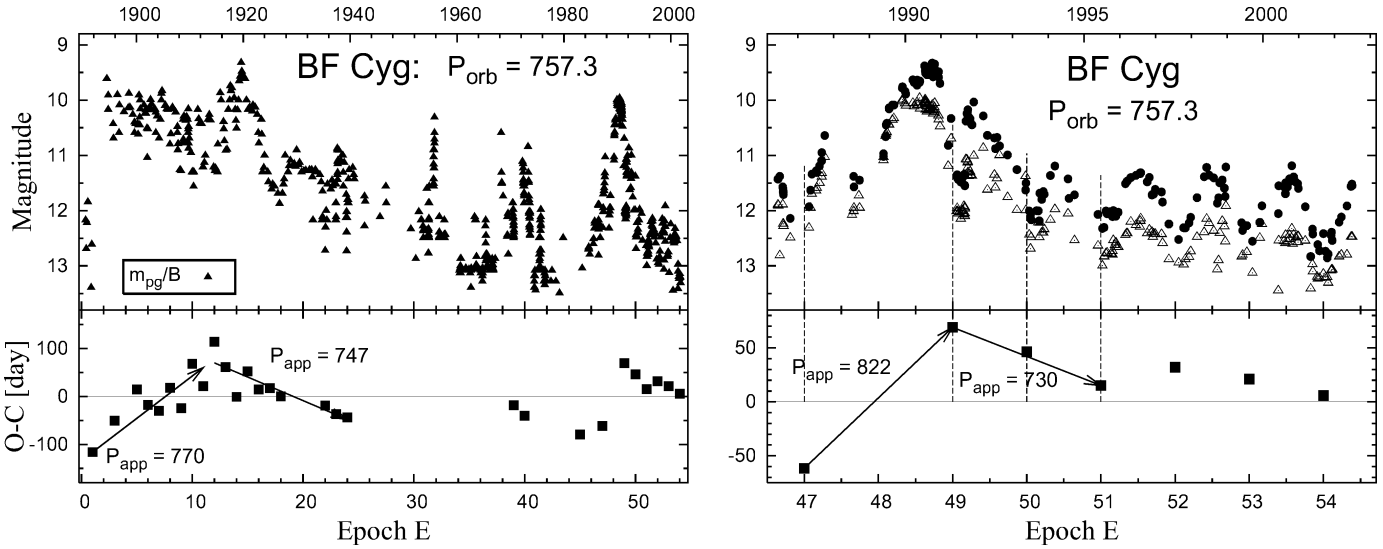

Figure 6. Historical and recent LCs of BF Cyg with the O–C diagrams. During transition from quiescent to active phases and vice versa, the main source of radiation contributing to the optical continuum changes significantly its location and geometry in the symbiotic system. As a result the observed minima change their profile and position, what we indicate in the O–C diagram as the apparent orbital changes.